Electronic Supplementary Material (ESI) for Journal of Materials Chemistry C.

Supporting Information

Enhanced photovoltaic efficiency and persisted photoresponse switchability in $LaVO_3/Pb(Zr_{0.2}Ti_{0.8})O_3$ perovskite heterostructures

Shengliang Cheng,[ab] Zhen Fan,*[ab] Lei Zhao,[ab] Haizhong Guo,[c] Dongfeng Zheng,[a] Zoufei Chen,[a] Min Guo,[a] Yue Jiang,[a] Sujuan Wu,[a] Zhang Zhang,[a] Jinwei Gao,[a] Xubing Lu,[a] Guofu Zhou,[bd] Xingsen Gao[a] and Jun-Ming Liu[ae]

[a]Institute for Advanced Materials, South China Academy of Advanced Optoelectronics, South China Normal University, Guangzhou 510006, China. E-mail: fanzhen@m.scnu.edu.cn

[b]Guangdong Provincial Key Laboratory of Optical Information Materials and Technology, South China Academy of Advanced Optoelectronics, South China Normal University, Guangzhou 510006, China

[c]School of Physical Engineering, Zhengzhou University, Zhengzhou 450001, China

[d]National Center for International Research on Green Optoelectronics, South China Normal University, Guangzhou 510006, China

[e]Laboratory of Solid State Microstructures and Innovation Center of Advanced Microstructures, Nanjing University, Nanjing 210093, China

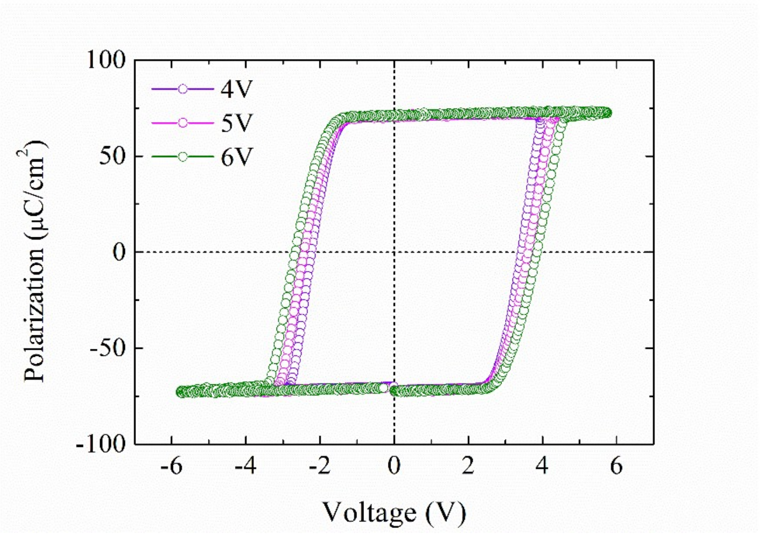

Figure S1. Evolution of *P*-*V* hysteresis loops with increasing applied $V_{\max}$ for the Pt/PZT/SRO capacitor.

The short saturation regime of the loop shown in Fig. 2f in the main text is caused by the relatively small applied $V_{\max}$ (i.e., 4 V), which is close to the voltage where the polarization switching is just completed. Applying $V_{\max}$ of >4 V may allow the polarization switching to be fully completed, resulting in a sharper loop (Fig. S1). However, increasing $V_{\max}$ to >4 V sometimes causes the sample breakdown. $V_{\max}$ = 4 V has therefore been used for our Pt/PZT/SRO capacitor in this work.

The growth of the LVO film on the PZT film is described as incoherent epitaxy, meaning that the two in-plane axes of the LVO lattice coincide with those of the PZT lattice but the LVO/PZT interface is not coherent. To support this viewpoint, the XRD φ and ω scans as well as TEM were performed, and the results are shown in Fig. S2-4, respectively.

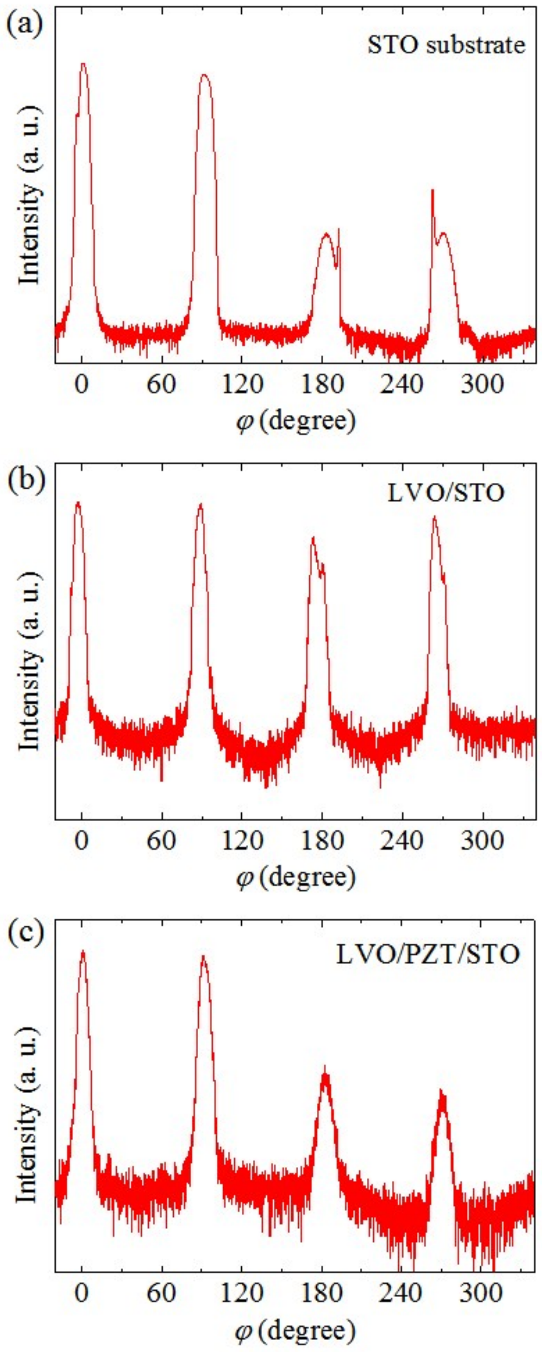

Figure S2. XRD *φ* scans for (a) STO substrate [@ STO (103)], (b) LVO/STO film [@ LVO (103)], and (c) LVO/PZT/STO film [@ LVO (103)].

For the XRD *φ* and *ω* scans, the following two LVO samples were used: the one grown directly on the STO substrate (LVO/STO) and the other grown on the PZT-buffered STO substrate (LVO/PZT/STO). As shown in the *φ* scans (Fig. S2), both LVO samples exhibit four peaks, which have the same positions as those of the STO substrate. Therefore, both LVO samples have the same in-plane orientational relationship with the STO substrate: LVO [100] // STO [100], suggesting the epitaxial growth of the LVO films on both bare STO and PZT-buffered STO substrates. The epitaxial qualities of the two LVO samples were further checked by the following *ω* scans (Fig. S3).

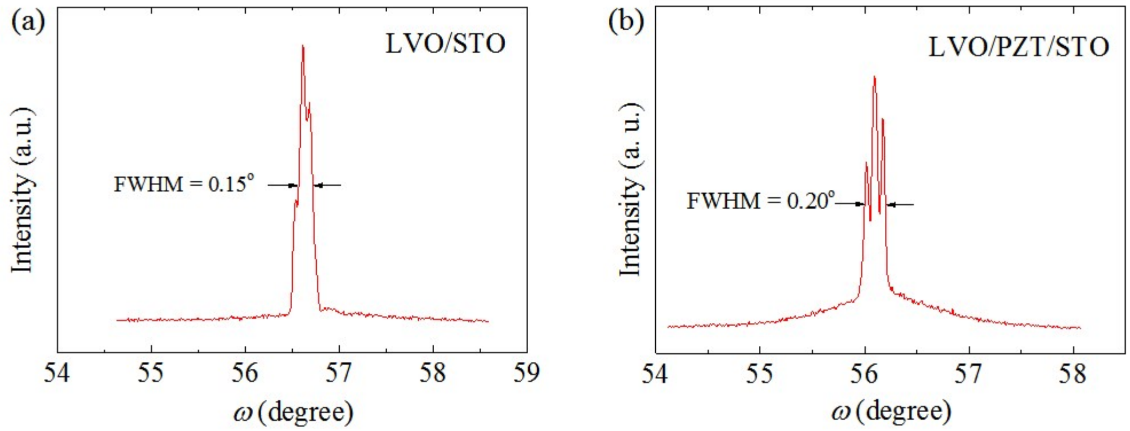

Figure S3. XRD ω scans of the LVO (103) peak for the (a) LVO/STO and (b) LVO/PZT/STO films. The intensity axis is in the linear scale.

Figure S3 shows that the full width at half maximum (FWHM) of the LVO (103) peak is 0.15° in the LVO/STO sample, but it increases to 0.20° in the LVO/PZT/STO sample. In addition, a wide hump emerges in the LVO/PZT/STO sample. These results suggest that the crystalline quality of LVO in the LVO/PZT/STO sample becomes poorer than that in the LVO/STO sample. The quality of the LVO/PZT interface was further checked by the following TEM (Fig. S4).

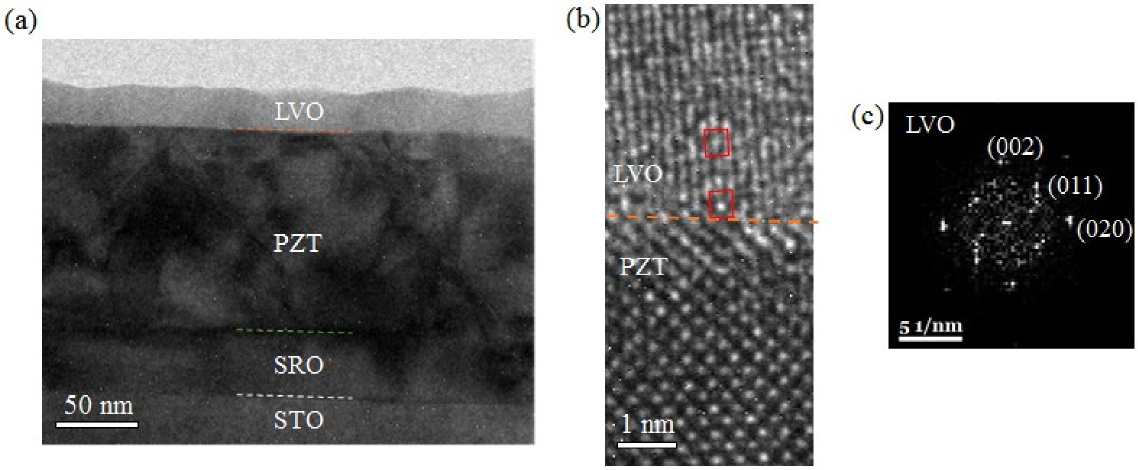

Figure S4. (a) Low-magnification TEM image of the LVO/PZT/SRO heterostructure on the STO substrate. (b) High-resolution TEM image of the LVO/PZT interfacial region. (c) Fast Fourier transform (FFT) pattern acquired in the LVO layer. In a and b, the dotted lines indicate the interfaces. In b, the red squares indicate the lattice of LVO.

Figure S4a shows that the three layers of LVO, PZT, and SRO are well grown with sharp interfaces. Figure S4b further shows that the LVO lattice is strongly distorted and the interface between LVO and PZT is not coherent, which may be caused by the following two factors. First, the growth of LVO on PZT is kind of incoherent epitaxy although their in-plane lattice parameters are quite close (~4 Å). Second, the perovskite structure of LVO has a poor thermodynamic stability[1], which may be distorted during the preparation of the TEM sample. Nevertheless, the vertical and horizontal lattice fringes of LVO can still be observed in Fig. S4b. By performing FFT in the LVO region, one can see the diffraction pattern corresponding to a perovskite phase (Fig. S4c). The out-of-plane and in-plane lattice parameters of LVO are calculated to be ~3.95 and ~3.91 Å, respectively, consistent with those obtained from the XRD results (Figs. 3a and b in the main text). Therefore, the combined TEM and XRD results confirm that the perovskite LVO film is successfully grown on the perovskite PZT film, in spite of the incoherent epitaxy.

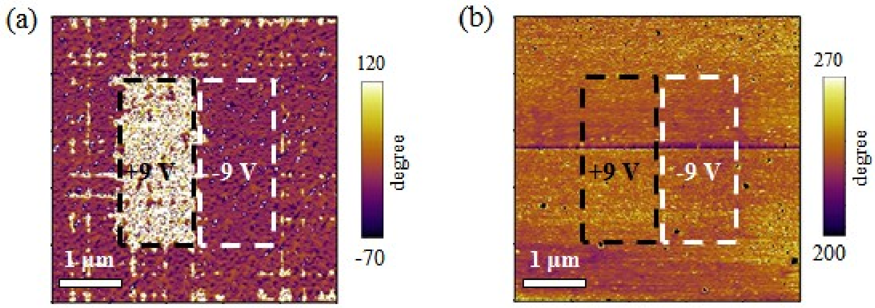

Figure S5. PFM phase images after electrical writing for the (a) LVO(24 nm)/PZT and (b) LVO(42 nm)/PZT films. The voltages of +9 V and -9 V are used for the positive and negative writing, respectively.

The comparison between Fig. S5 and Fig. 2d in the main text demonstrates that the domains can be fully switched in the LVO/PZT film when d_{LVO} is no larger than 24 nm.

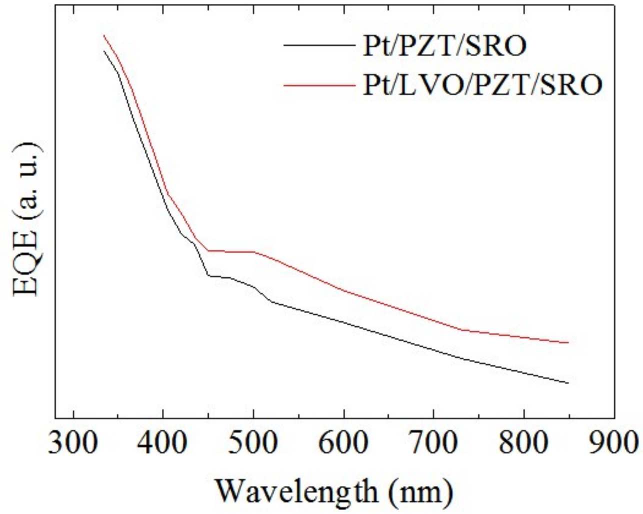

Figure S6. EQE spectra for the Pt/LVO(24 nm)/PZT/SRO and Pt/PZT/SRO devices.

As shown in Fig. S6, the EQEs of the Pt/LVO/PZT/SRO device are larger than those of the Pt/PZT/SRO device in the whole wavelength region of 330-850 nm, and the EQE enhancements are more observable in the 450-850 nm region than in the 330-450 nm region. Based on the following equation:

$$I_{\mathrm{sc}}=\int A\cdot q\cdot \mathrm{EQE}(\lambda)\cdot N(\lambda)\,\mathrm{d}\lambda, \tag{S1}$$

where A is the electrode area, q is the electron charge, λ is the light wavelength, and N is the number density of incident photons for the AM1.5G spectrum, the I_{sc} of the Pt/LVO/PZT/SRO device is estimated to be ~2 times as large as that of the Pt/PZT/SRO device, consistent with the results in Fig. 5 in the main text. It is therefore confirmed that the PV performance is indeed enhanced by integrating the LVO film (24 nm) with the PZT film.

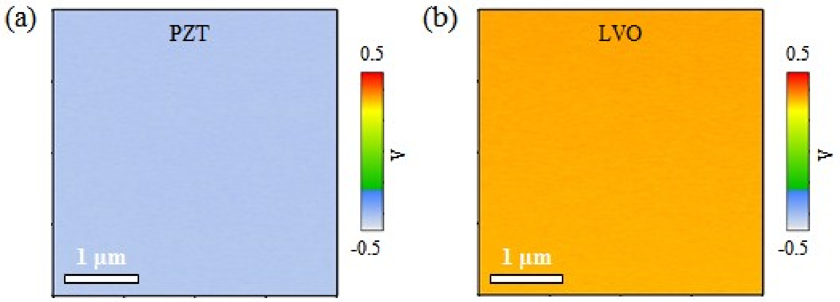

Figure S7. Surface potential maps of the (a) PZT and (b) LVO films.

The surface potential of the LVO film is ~0.7 V higher than that of the PZT film, suggesting that the work function (Φ) of the former is ~0.7 eV smaller than that of the latter. This work function difference is consistent with the theoretical value (Φ_{LVO} = ~4.0 eV[2,3] and Φ_{PZT} = 4.6 eV[4,5]).

References

1. R.Pankajavalli and O.M.Sreedharan, Mater. Lett., 1995, 24, 247–251

2. L. Wang, Y. Li, A. Bera, C. Ma, F. Jin, K. Yuan, W. Yin, A. David, W. Chen, W. Wu, W. Prellier, S. Wei and T. Wu, Phys. Rev. Appl., 2015, 3, 064015.

3. M. Jellite, J. Rehspringer, M. Fazio, D. Muller, G. Schmerber, G. Ferblantier, S. Colis, A. Dinia, M. Sugiyama, A. Slaoui, D. Cavalcoli and T. Fix, Solar Energy, 2018, 162, 1–7.

4. D. Cao, C. Wang, F. Zheng, W. Dong, L. Fang and M. Shen, Nano Lett., 2012, 12, 2803–2809.

5. F. Zheng, Y. Xin, W. Huang, J. Zhang, X. Wang, M. Shen, W. Dong, L. Fang, Y. Bai, X. Shen and J. Hao, J. Mater. Chem. A, 2014,2, 1363–1368.